Inorg. Chem. **2003**, *42*, 7809–7818

Synthesis and Structural Characterization of Double Metal Cyanides of Iron and Zinc: Catalyst Precursors for the Copolymerization of Carbon Dioxide and Epoxides

Donald J. Darensbourg,* M. Jason Adams, Jason C. Yarbrough, and Andrea L. Phelps

Department of Chemistry, Texas A&M University, College Station, Texas 77843

Received July 8, 2003

Several synthetic approaches for the preparation of double metal cyanide (DMC) derivatives of iron(II) and zinc(II) are described. These include (1) metathesis reactions of $ZnCl_2$ or ZnI_2 with $KCpFe(CN)_2CO$ in aqueous solution, (2) reactions of $KCpFe(CN)_2CO$ and its phosphine-substituted analogues with $Zn(CH_3CN)_4(BF_4)_2$ and subsequent displacement of acetonitrile at the zinc centers by the addition of a neutral (phosphine) or anionic (phenoxide) ligand, and (3) reactions of the protonated $HCpFe(CN)_2$(phosphine) complexes with $Zn(N(SiMe_3)_2)_2$, followed by the addition of phenols. All structures are based on a diamond-shaped planar arrangement of the $Fe_2(CN)_4Zn_2$ core with various appended ligands at the metal sites. Although attempts to replace the iodide ligands in $[CpFe(\mu\text{-}CN)_2PPh_3ZnI(THF)]_2$ with acetate using silver acetate failed, two novel cationic mixed-metal cyanide salts based on the $[CpFe(PPh_3)(\mu\text{-}CN)_2Zn(NC_5H_5)]_2^{2+}$ framework were isolated from pyridine solution and their structures were defined by X-ray crystallography. The anionic ligand bound to zinc in these derivatives, which serve as an anionic polymerization initiator, was shown to be central to the catalytic copolymerization reaction of CO_2/epoxide to provide polycarbonates and cyclic carbonates. The structurally stabilized phosphine-strapped complexes $[CpFe(\mu\text{-}CN)_2Zn(X)THF]_2(\mu\text{-dppp})$, where X = I or phenolate, were shown to be thermally stable under the conditions (80 °C) of the copolymerization reaction by in situ infrared spectroscopy. Both of these derivatives were proposed to serve as mimics for the heterogeneous DMC catalysts in the patent literature, with the derivative where the initiator is a phenolate being more active for the production of polycarbonates.

Introduction

The metal-catalyzed copolymerization of carbon dioxide and epoxides to produce biodegradable polycarbonates offers an economical and environmentally benign alternative to the current industrially practiced method for their preparation. This latter methodology involves the biphasic polycondensation of phosgene (or one of its derivatives) and a diol.[1] Much recent research activity has been directed at the design of well-characterized transition metal complexes as homogeneous catalysts or catalyst precursors for the copolymerization of carbon dioxide and cyclohexene oxide to produce poly(cyclohexylene carbonate).[2] Unfortunately, these well-defined catalysts are in general much less effective at copolymerizing carbon dioxide and propylene oxide, instead producing cyclic propylene carbonate. However, in some

* To whom correspondence should be addressed. E-mail: djdarens@mail.chem.tamu.edu. Fax: (979) 845-0158.

(1) *Engineering Thermoplastics: Polycarbonates, Polyacetals, Polyesters, Cellulose Esters*; Bottenbruch, L., Ed.; Hanser Pub.: New York, 1996; p 112.

(2) (a) Darensbourg, D. J.; Holtcamp, M. W. *Macromolecules* **1995**, *28*, 7577−7579. (b) Kruper, W. J.; Dellar, D. V. *J. Org. Chem.* **1995**, *60*, 725−727. (c) Super, M.; Berluche, E.; Costello, C.; Beckman, E. *Macromolecules* **1997**, *30*, 368−372. (d) Super, M.; Beckman, E. J. *Macromol. Symp.* **1998**, *127*, 89−108. (e) Cheng, M.; Lobkovsky, E. B.; Coates, G. W. *J. Am. Chem. Soc.* **1998**, *120*, 11018−11019. (f) Beckman, E. *Science* **1999**, *283*, 946−947. (g) Darensbourg, D. J.; Holtcamp, M. W.; Struck, G. E.; Zimmer, M. S.; Niezgoda, S. A.; Rainey, P.; Robertson, J. B.; Draper, J. D.; Reibenspies, J. H. *J. Am. Chem. Soc.* **1999**, *121*, 107−116. (h) Nozaki, K.; Nakano, K.; Hiyama, T. *J. Am. Chem. Soc.* **1999**, *121*, 11008−11009. (i) Darensbourg, D. J.; Wildeson, J. R.; Yarbrough, J. C.; Reibenspies, J. H. *J. Am. Chem. Soc.* **2000**, *122*, 12487−12496. (j) Cheng, M.; Darling, N. A.; Lobkovsky, E. B.; Coates, G. W. *Chem. Commun.* **2000**, 2007−2008. (k) Inoue, S. *J. Polym. Sci., Part A* **2000**, *38*, 2861−2871. (l) Mang, S.; Cooper, A. I.; Colclough, M. E.; Chauhan, N.; Holmes, A. B. *Macromolecules* **2000**, *33*, 303−308. (m) Cheng, M.; Moore, D. R.; Reczek, J. J.; Chamberlain, B. M.; Lobkovsky, B. E.; Coates, G. W. *J. Am. Chem. Soc.* **2001**, *123*, 8738−8749. (n) Darensbourg, D. J.; Yarbrough, J. C. *J. Am. Chem. Soc.* **2002**, *124*, 6335−6342. (o) Eberhardt, R.; Allmendinger, M.; Luinstra, G. A.; Rieger, B. *Organometallics* **2003**, *22*, 211−214. (p) Eberhardt, R.; Allmendinger, M.; Rieger, B. *Macromol. Rapid Commun.* **2003**, *24*, 194−196.

10.1021/ic0347900 CCC: $25.00
Published on Web 11/01/2003

instances it is possible to enhance the rate of polypropylene carbonate production over cyclic propylene carbonate by carrying out the process at lower temperatures.[3,4]

The patent literature contains numerous references demonstrating that double metal cyanides (DMC) of the general formula $[M^a]_m[M^b(CN)_6]_n$, where M^a is a oxophilic metal and M^b is a transition metal, show great promise for the coupling of propylene oxide or ethylene oxide and carbon dioxide.[5] Among catalysts of this composition, zinc hexacyanoferrate(III) has been particularly effective. *It is noteworthy to state here that the generally very high activity achieved by these catalysts for both poly(ether polyol)s and polycarbonate production is profoundly dependent on the details of the activation steps of these heterogeneous catalysts.*[6] Nevertheless, there is one report in the open literature which describes an active cobalt or nickel cyanide/zinc catalyst for the synthesis of poly(ether polyol)s which appears to be less sensitive to the method of catalyst activation.[7] Despite their impressive activity for homopolymerization of epoxides or copolymerization of epoxide/CO_2, these DMC catalysts are poorly understood with respect to structure and reaction pathway.

Herein, we wish to communicate our early findings aimed at providing a better understanding of the role of double metal cyanides of iron and zinc in the copolymerization process of carbon dioxide and epoxides. These studies involve the synthesis and characterization of several well-defined, mixed-metal cyanide derivatives of iron(II) and zinc(II), along with an examination of their reactivity toward the CO_2/epoxides coupling reaction.[8]

Results and Discussion

Our initial investigations into the synthesis of double metal cyanides of iron and zinc began with the reaction of [K][$CpFe(CN)_2CO$] (**1**) with $ZnCl_2$ in water.[8] This reaction was performed by the dropwise addition of an aqueous solution of **1** to 1 equiv of $ZnCl_2$ in water with vigorous stirring. The yellow powder isolated from this reaction was insoluble in water and all common organic solvents. Elemental analysis of this material proved it to be the simple product of a metathesis reaction (eq 1), where zinc had replaced potassium as the counterion to the $CpFe(CN)_2CO$ anion. The identical product was obtained from the reactions of **1** and ZnI_2 in water or **1** and $ZnCl_2$ in acetonitrile. The solid-state (KBr) infrared spectrum of [Zn][$CpFe(CN)_2CO]_2$ (**2**) exhibited two

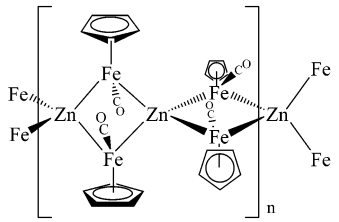

Figure 1. Proposed structure of [$CpFe(CO)(\mu$-$CN)_2]_2$[Zn], where bridging cyanides are drawn as lines for clarity.

cyanide and two carbonyl stretching vibrations at 2139 and 2119 cm^{-1} and 1986 and 1973 cm^{-1}, respectively. The observation that the two ν(CN) values are shifted to higher frequency when compared with those of **1** (2085 and 2095 cm^{-1}) is strongly indicative of *both* cyanide ligands being coordinated in bridging modes, i.e., of the form Fe−C≡N−Zn. Nevertheless, this is not necessarily the case, and other techniques would be essential to definitively describe the nature of the cyanides bonding modes.

$$2[K][CpFe(CN)_2CO] + ZnCl_2 \xrightarrow{\text{water}} \underset{\text{insoluble precipitate}}{[Zn][CpFe(CN)_2CO]_2} + 2KCl \quad (1)$$

After exhaustive attempts of carrying out reaction 1 under varying reaction conditions in an effort to provide single crystals of **2** suitable for X-ray crystallography failed, we have undertaken solid-state ^{13}C and ^{15}N NMR studies to better define the structure of complex **2**. The ^{13}C resonance due to the cyanide ligands in **2** was observed at 158.3 ppm, or about 15.9 ppm upfield from the parent complex **1**. Furthermore, the ^{15}N NMR spectrum of **2** exhibited a single chemical shift for the two cyanide ligands at 251.7 ppm, which is shifted downfield from **1** by 64.9 ppm. Hence, the solid-state NMR results definitively show the two cyanide ligands to be in the same magnetic environment or to be chemically equivalent. On the basis of the ν(CN) and ^{13}C/^{15}N NMR data, coupled with the elemental analysis (i.e., Fe:Zn of 2:1 and <0.3% Cl), **2** is assigned the structure shown in Figure 1. The proposed structure of **2** bears a close resemblance to that found for the zeolitic zinc ferrocyanide, $Na_2Zn_3[Fe(CN)_6]_2 \cdot nH_2O$.[9] The basic structure of this network solid can be described as octahedral FeC_6 units surrounded by tetrahedral ZnN_4 units, with sodium ions and water molecules filling the interstitial cavities.

Although complex **2** lacked the desired solubility to serve as a homogeneous catalyst, the copolymerization of propylene oxide and carbon dioxide was undertaken with **2** employed as a heterogeneous catalyst for this process. Complex **2** was activated in a manner similar to that described in the patent literature.[6] That is, **2** was homogenized in degassed *tert*-butyl alcohol. This was followed by a water wash and a second homogenization step using *tert*-butyl alcohol and poly(propylene glycol) monobutyl ether. The resulting slurry was filtered through a 4−5.5 μm filter

(3) Darensbourg, D. J.; Yarbrough, J. C.; Ortiz, C.; Fang, C. C. *J. Am. Chem. Soc.* **2003**, *125*, 7586−7591.
(4) Allen, S. D.; Moore, D. R.; Lobkovsky, E. B.; Coates, G. W. *J. Am. Chem. Soc.* **2002**, *124*, 14284−14285.
(5) (a) Kruper, W. J., Jr.; Swart, D. J. U.S. Patent 4,500,704, 1985. (b) There is also a similar report in the open literature: Chen, L.-B. *Makromol. Chem. Macromol. Symp.* **1992**. *59*, 75−82.
(6) (a) Milgrom, J. U.S. Patent 3,427,256, 1969. (b) Le-Khac, B. U.S. Patent 5,482,908, 1996. (c) Ooms, P.; Hofmann, J.; Gupta, P.; Groenendaal, L U.S. Patent 6,204,357, 2001. (d) Le-Khac, B. U.S. Patent 6,211,330, 2001. (e) Hofmann, J.; Ooms, P.; Gupta, P.; Schafer, W. U.S. Patent 6,291,388, 2001.
(7) Garcia, J. L.; Jang, E. J.; Alper, H. *J. Appl. Polym. Sci.* **2002**, *86*, 1553−1557.
(8) Darensbourg, D. J.; Adams, M. J.; Yarbrough, J. C. *Inorg. Chem.* **2001**, *40*, 6543−6544.
(9) (a) Gravereau, P.; Garnier, E.; Hardy, A. *Acta Crystallogr.* **1979**, *B35*, 2843−2848. (b) Garnier, E.; Gravereau, P.; Hardy, A. *Acta Crystallogr.* **1982**, *B38*, 1401−1405.

Table 1. IR and ^{31}P NMR Data for Compounds **2**−**7**

compd	condition	ν(CN), cm^{-1}	ν(CO), cm^{-1}	δ, ppm
[CpFe(CO)(μ-CN)$_2$]$_2$[Zn] (**2**)	KBr	2139, 2119	1986, 1973	
[CpFe(CO)(μ-CN)$_2$ZnI(CH$_3$CN)]$_2$ (**3**)	CH$_3$CN	2134, 2124	1982	
[CpFe(CO)(μ-CN)$_2$Zn(PPh$_2$Me)(CH$_3$CN)]$_2$[BF$_4$]$_2$ (**4**)	CH$_3$CN	2131, 2118	1992	−21.8
[CpFe(CO)(μ-CN)$_2$Zn(PCy$_3$)(CH$_3$CN)]$_2$[BF$_4$]$_2$ (**5**)	CH$_3$CN	2135, 2120	1986	29.6, 11.8
[CpFe(CO)(μ-CN)$_2$Zn(P(^{t}Bu)$_3$)(CH$_3$CN)]$_2$[BF$_4$]$_2$ (**6**)	CH$_3$CN	2133, 2118	1987	37.3, 31.0
[CpFe(CO)(μ-CN)$_2$Zn(2,4,6-OC$_6$H$_2$(CH$_3$)$_3$)(CH$_3$CN)]$_2$ (**7**)	THF	2139, 2126	1985	a

[a] ^{1}H NMR chemical shifts for **7** are as follows: 2.19 (s), 2.21 (s), and 6.78 (s) ppm.

frit and dried overnight in a vacuum oven at 80 °C to provide the activated catalyst derived from complex **2**. The copolymerization attempt utilizing this catalyst produced little polypropylene carbonate, instead yielding most cyclic propylene carbonate as evidenced by its ν(CO$_2$) band at 1799 cm^{-1}, which was approximately one-third as intense as the ν(CO$_2$) absorption of the copolymer at 1749 cm^{-1}. Although these observations are less than extraordinary, they do indicate that complex **2** exhibits reactivity properties in common with the heterogeneous double metal cyanides in the patent literature.

Since the goal of this research is to prepare well-characterized DMC catalysts, thus requiring no preactivation steps, a soluble double metal cyanide (DMC) of iron and zinc was prepared upon reacting ZnI$_2$ with KCpFe(CN)$_2$CO in acetonitrile (instead of water) to afford complex **3**, [CpFe(CO)(μ-CN)$_2$ZnI(CH$_3$CN)]$_2$. Alternatively, it was possible to inhibit the formation of metal aggregate and afford soluble DMC derivatives by adding phosphines to Zn(CH$_3$CN)$_4$(BF$_4$) prior to reacting it with KCpFe(CN)$_2$CO in acetonitrile. In this manner the cationic PPh$_2$Me (**4**), PCy$_3$ (**5**), and P^{t}Bu$_3$ (**6**) derivatives were synthesized. Table 1 lists the ν(CN) and ν(CO) infrared data, as well as the ^{31}P NMR data for all of the complexes prepared. In general the ^{31}P NMR signals are broad in complexes **4**−**6**, indicative of exchange between bound and free phosphine groups.

Anionic ligands, such as phenoxide, bound to zinc may protect it from affording aggregate double metal cyanides with KCpFe(CN)$_2$CO. Indeed, this was achieved by the addition of 1 equiv of KCpFe(CN)$_2$CO to a solution of the *mono*(phenoxide) derivative of zinc which was prepared from the reaction of anhydrous zinc chloride and sodium 2,4,6-trimethylphenoxide in acetonitrile. The absence of the very stable bis(phenoxide) derivative of zinc was visually observed since it is insoluble under these conditions.[2g] As noted in the case of the cationic phosphine derivatives, the ν(CN) and ν(CO) frequencies were shifted to higher wavenumbers compared to the parent potassium salt (**1**). The ^{1}H NMR spectrum of this phenoxide derivative, complex **7**, [CpFe(CO)(μ-CN)$_2$Zn(2,4,6-OC$_6$H$_2$(CH$_3$)$_3$)(CH$_3$CN)]$_2$, shows methyl singlets at 2.19 and 2.21 ppm and an aromatic singlet at 6.78 ppm.

Because of the lack of thermal stability (e.g., dissociation of CO ligand) under the conditions of the copolymerization process of these latter soluble carbonyl derivatives of DMCs (complexes **2**−**7**), we have directed our attention at synthesizing more stable phosphine complexes. This was accomplished by employing phosphine-substituted derivatives of KCpFe(CN)$_2$L or [KCpFe(CN)$_2$]$_2$L$_2$, where L = monophosphine and L$_2$ = diphosphine.[10] The reaction of ZnI$_2$ with KCpFe(CN)$_2$PPh$_3$ in acetonitrile provided the complex [CpFe(PPh$_3$)(μ-CN)$_2$ZnI(THF)]$_2$ (**8**) in good yield upon isolation from a THF solution. As expected, the ν(CN) vibrations of the parent KCpFe(CN)$_2$PPh$_3$ species shift to higher wavenumbers upon complexation with zinc. Furthermore, these vibrational modes are significantly lower in frequency at 2092 and 2082 cm^{-1} than those of the CO analogue [CpFe(CO)(μ-CN)$_2$ZnI(THF)]$_2$, which appear at 2134 and 2124 cm^{-1}. Presumably, this is a reflection of enhanced interaction of the nitrogen centers with zinc in complex **8**, thereby accounting for its greater thermal stability. Single crystals of complex **8** were obtained from a THF/hexane solution. However, these crystals were of poor quality and only led to a structural solution with an *R* value of 20.8%. Nevertheless, the atom connectivity was adequately defined indicating the iron and zinc metal centers are linked by cyanide ligands. This structure is also consistent with infrared and NMR spectral data in solution, as well as elemental analysis. A ball-and-stick representation of the structure is depicted in Figure 2.

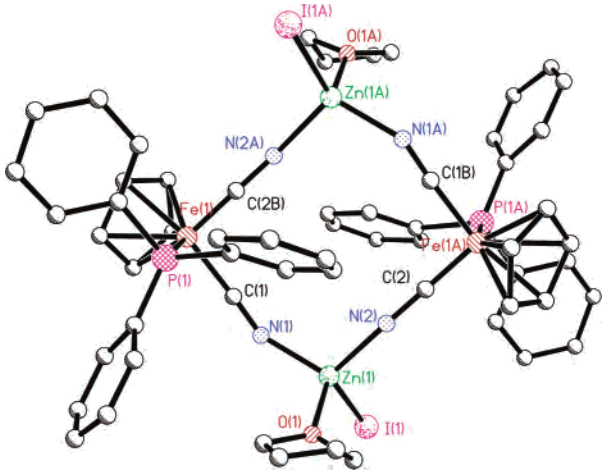

Figure 2. Ball-and-stick drawing of complex **8**, [CpFe(PPh$_3$)(μ-CN)$_2$ZnI(THF)]$_2$.

A mixed-metal cyanide complex similar to **8** containing slightly lower ν(CN) vibrational modes at 2088 and 2080 cm^{-1} was synthesized from KCpFe(CN)$_2$PPh$_3$ and Zn(CH$_3$CN)$_4$(BF$_4$)$_2$ in acetonitrile. This derivative, [CpFe(PPh$_3$)(μ-CN)$_2$Zn(CH$_3$CN)$_2$BF$_4$]$_2$ (**9**), is potentially a convenient route to substitute other anions for BF$_4^-$, such as alkoxides or phenoxides. These latter nucleophiles are good initiators for the copolymerization reaction involving

(10) Darensbourg, D. J.; Adams, M. J.; Yarbrough, J. C.; Phelps, A. L. *Eur. J. Inorg. Chem.* **2003**, 3639−3648.

Table 2. Infrared (ν(CN)) and ^{31}P NMR Spectral Data for Complexes **8**−**16**

compd	condition	ν(CN), cm^{-1}	δ, ppm
$[CpFe(PPh_3)(\mu\text{-}CN)_2ZnI(THF)]_2$ (**8**)	CH_3CN	2092, 2082	
	THF	2091, 2082	81.4
$[CpFe(PPh_3)(\mu\text{-}CN)_2Zn(BF_4)(CH_3CN)]_2$ (**9**)	CH_3CN	2088, 2080	80.6
$[\{CpFe(PPh_3)(\mu\text{-}CN)_2Zn(NC_5H_5)\}_2\{CpFe(PPh_3)(\mu\text{-}CN)_2\}_2ZnI(NC_5H_5)][AgI_2]$ (**10a**)	KBr	2088, 2084, 2072, 2063	
$[CpFe(\mu\text{-}CN)_2(PPh_3)Zn(NC_5H_5)_2]_2[AgI_2]_2$ (**10b**)	KBr	2081, 2062	
	pyridine	2091, 2081	81.6
$[CpFe(\mu\text{-}CN)_2ZnI(THF)]_2(\mu\text{-dppp})$ (**11**)	THF	2088, 2082 (sh)	71.8
$[CpFe(\mu\text{-}CN)_2Zn(BF_4)(THF)]_2(\mu\text{-dppp})$ (**12**)	CH_3CN	2086, 2082 (sh)	70.52
$H[CpFe(PPh_3)(CN)_2]$ (**13**)	KBr	2102, 2068	81.5[a]
$[HCpFe(CN)_2]_2(\mu\text{-dppp})$ (**14**)	KBr	2101, 2083	
$[CpFe(PPh_3)(\mu\text{-}CN)_2Zn(2,6\text{-}OC_6H_3(tert\text{-butyl})_2)(THF)]_2$ (**15**)	THF	2101, 2080	
$[CpFe(\mu\text{-}CN)_2Zn(2,6\text{-}OC_6H_3(tert\text{-butyl})_2)(THF)]_2(\mu\text{-dppp})$ (**16**)	THF	2101, 2078	

[a] In methanol solvent.

carbon dioxide and epoxides. The BF_4^- anion is most likely interacting at the zinc center as inferred from the similarity of the ν(CN) vibrational modes in compounds **8** and **9**. Table 2 contains ν(CN) and ^{31}P NMR data for the mixed-metal iron phosphine complexes prepared in this study.

In an alternate approach to preparing double metal cyanides with other anionic nucleophiles bound to the zinc centers, we have reacted complex **8** with silver acetate. A precipitate of AgI was readily evident upon reacting complex **8** with 2 equiv of silver acetate. Following solvent removal via vacuum, the resulting yellow solid was dissolved in pyridine and the solution allowed to stand at ambient temperature with slow evaporation of pyridine leading to crystals of complex **10a**, $[\{CpFe(PPh_3)(\mu\text{-}CN)_2Zn(NC_5H_5)\}_2\{CpFe(PPh_3)(\mu\text{-}CN)_2\}_2ZnI(NC_5H_5)][AgI_2]$. The solid-state infrared spectrum of the single crystals of **10a** displayed a broad ν(CN) region with bands at 2088, 2084, 2072, and 2063 cm^{-1}. Upon further standing, the pyridine solution afforded another set of single crystals, complex **10b**, $[CpFe(\mu\text{-}CN)_2(PPh_3)Zn(NC_5H_5)_2]_2[AgI_2]_2$, which exhibited a much simpler ν(CN) solid-state spectrum with absorptions at 2081 and 2062 cm^{-1}.

Because of the complicated nature of the infrared spectrum of complex **10a**, it was of particular importance to structurally characterize this derivative via X-ray crystallography. Unfortunately, due to several factors, including the quality of the isolated crystals, the structure of **10a** was only refined to an *R* value of 18.4%. Nevertheless, the crystal structure is of sufficient quality with a goodness-of-fit parameter of 1.161 to well-define the important features of the structure. As depicted in Figure 3, complex **10a** was found to consist of polymeric double metal cyanide chains comprised of zinc/iron cyanide diamonds connected by bridged iron−zinc linkages. The coordination sphere of zinc in the diamond was completed by a pyridine molecule, where in the bridge by both pyridine and iodide ligands. This polymeric chain propagates in an undulating fashion due to the bends at the bridging units. Silver diiodide serves as the counterion for the complex, which along with solvent molecules has been omitted from Figure 3 for clarity.

The second batch of crystals obtained from the reaction of complex **8** with silver acetate in pyridine provided the structure illustrated in Figure 4. For descriptive purposes this complex, **10b**, can be thought to be derived from **10a** by a

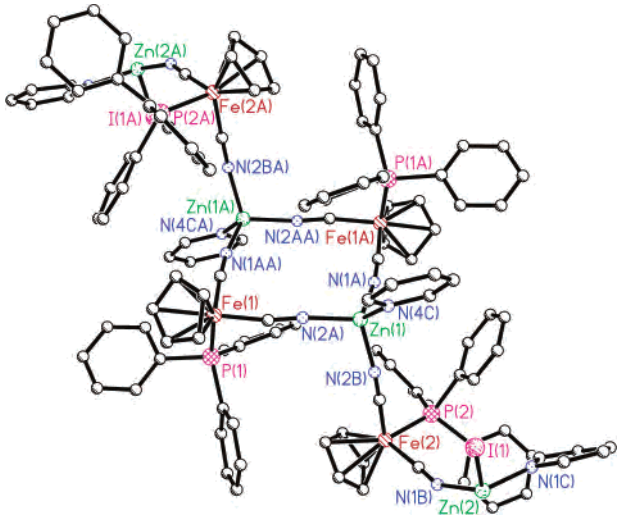

Figure 3. Ball-and-stick representation of the structure of complex **10a**.

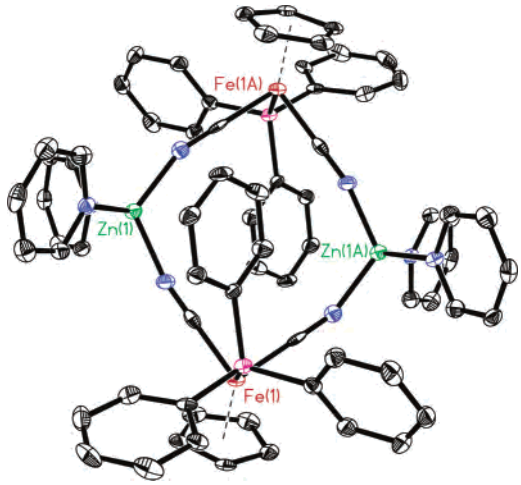

Figure 4. Thermal ellipsoid plot of $[CpFe(\mu\text{-}CN)_2(PPh_3)Zn(NC_5H_5)_2]_2[AgI_2]_2$ (**10b**), with hydrogen atoms and anions removed for clarity.

ligand substitution process at the zinc centers of the diamond structure. That is, replacement of the ···NC−FeCp(PPh$_3$)-CN ligand in complex **10a** by pyridine leads to the dicationic complex **10b**. As seen in all the complexes reported upon herein and elsewhere, the Fe−C−N angles deviate only slightly from 180° (Table 3), whereas, the C−N−Zn angles are far from linearity at 163.4 and 157.7°. It is interesting that these cyanide bridges are not symmetric, which allows one of them to form a more linear orientation at the expense

Table 3. Selected Bond Distances (Å) and Angles (deg) for $[CpFe(\mu\text{-}CN)_2(PPh_3)Zn(NC_5H_5)_2]_2[AgI_2]_2$, **10b**, and $[CpFe(\mu\text{-}CN)_2ZnI(THF)_2](\mu\text{-dppp})$, **11**[a]

		Complex **10b**	
Fe(1)−C(1)	1.849(4)	Fe(1)−C(1)−N(1)	178.6(3)
Fe(1)-C(2)	1.847(4)	Fe(1)−C(2)−N(2)	176.8(3)
Zn(1)−N(1)	1.927(3)	Zn(1)−N(1)−C(1)	163.4(3)
Zn(2)−N(2)	1.931(3)	Zn(1)−N(2)−C(2)	157.7(3)
Zn(1)−N(3)	2.023(3)	N(1)−Zn(1)−N(2)	118.43(13)
Zn(1)−N(4)	2.025(3)	N(3)−Zn(1)−N(4)	112.76(12)
		Fe(1)−C(1)−N(1)	178.6(3)
		Complex **11**	
Fe(1)−C(1)	1.838(10)	Fe(1)−C(1)−N(1)	178.6(9)
Fe(1)−C(2)	1.851(11)	Fe(1)−C(2)−N(2)	178.5(9)
Zn(1)−N(1)	1.943(8)	Zn(1)−N(1)−C(1)	156.0(8)
Zn(2)−N(2)	1.946(8)	Zn(2)−N(2)-C(2)	167.9(7)
Zn(1)−O(1)	2.058(10)	N(1)−Zn(1)−N(1A)	110.8(5)
Zn(2)−O(2)	2.046(5)	N(2)−Zn(2)−N(2A)	106.5(4)
		I(1)−Zn(1)−O(1)	106.7(3)
		I(2)−Zn(2)−O(2)	119.7(2)

[a] Estimated standard deviations are given in parentheses.

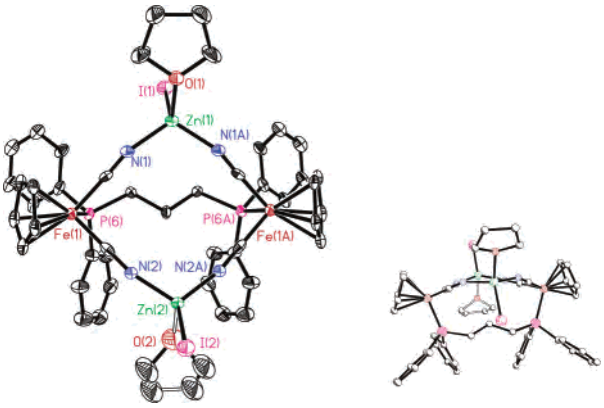

Figure 5. Thermal ellipsoid plot of $[CpFe(\mu\text{-}CN)_2ZnI(THF)]_2(\mu\text{-dppp})$ (**11**) with the a side view inset provided for clarity.

of the other. The bond angle of N(1)−Zn(1)−N(2) is quite large at 118°, with the angle formed by the zinc and pyridine ligands being closer to tetrahedral at 112°. Albeit that complexes **10a,b** possess interesting structural features (polymeric chain structure of **10a** and cationic diamond structure of **10b**) not previously observed, it is apparent that the synthetic methodology of replacing a zinc-bound halide with the anion from a soluble silver salt is fraught with complications. Therefore, other preparative approaches will need to be explored.

Since the copolymerization reaction of epoxides and carbon dioxide is generally carried out at temperatures greater than 60 °C, it is desirable to have thermally robust iron/zinc double metal cyanide derivatives as catalysts. To achieve this goal we have employed the phosphine bridged diiron species, $[CpFe(CN)_2PPh_2(CH_2)_3PPh_2Fe(CN)_2Cp]^{2-}$, which can serve as a single side strapping to hold the structure intact during the catalytic reaction. Complex **11**, $[CpFe(\mu\text{-}CN)_2ZnI(THF)]_2(\mu\text{-dppp})$, was prepared from the reaction of the bridging diiron dianion and ZnI_2 in acetonitrile following isolation and recrystallization from THF.[8] The X-ray derived crystal structure of complex **11** may be seen in Figure 5.

The effects of bridging the iron centers in **11** can be seen in the metric data for the metallocycle unit. This basket-shaped molecule displays a nonplanar $[Fe(CN)_2Zn]_2$ geometry, which is largely due to the restrictive length of the phosphine bridge. The resulting puckered ring provides two unique zinc environments, as a result of one of the zinc atoms greater deviation from linearity in the cyanide bridge. Furthermore, the nature of the bridging phosphine relegates both phosphine groups to the same face of the metallocycle. This is a significant departure from the nonbridged double metal cyanides, which all form the more symmetric and less sterically hindered complexes with substituents on opposite faces of the ring. Consistent with these structural observations we were unable to prepare the analogous complex using the $[KCpFe(CN)_2)]_2(\mu\text{-dppe})$ salt, whereas, extending the phosphine bridge to dppb ((diphenylphosphino)butane) readily allowed for the synthesis of an analogue of complex **11**.

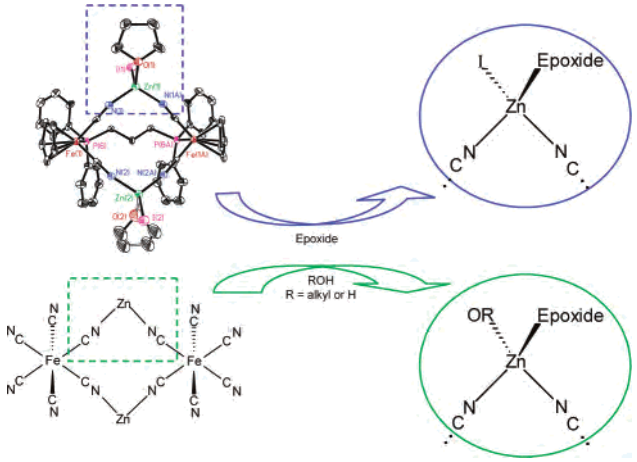

Figure 6. Comparative illustration of catalytically active zinc site in **11** (top) and heterogeneous (bottom) systems.

The structural parameters observed in complex **11** are quite similar to the corresponding bond distances and angles in $Na_2Zn_3[Fe(CN)_6]_2\cdot 9H_2O$.[9] For example, selected bond lengths (Å) and angles (deg) in complex **11** of Fe−C 1.838(10), Zn−N 1.945(8)Å, Fe−C−N 178.6(9), Zn−N−C 156.0(8) and 167.9(7), and N−Zn−N 110.8(5) compare well with the analogous values in $Na_2Zn_3[Fe(CN)_6]_2\cdot 9H_2O$: Fe−C 1.881(3), Zn−N 1.9685(7), Fe−C−N 178.8(7), Zn−N−C 159.7(6), N−Zn−N 110(4). These results indicate that the model double metal cyanide derivative, complex **11**, is structurally comparable to the activated form of the heterogeneous DMC catalysts found in the patent literature.[6] Furthermore, the coordinated THF ligands have been shown to have binding affinities to zinc only slightly greater than those of epoxides.[11] Therefore, the dissolution of **11** in liquid epoxides should lead directly to the formation of the activated epoxide complex. This is illustrated in Figure 6, where the most significant difference between the active zinc centers in the homogeneous and heterogeneous catalysts systems is the poorer epoxide ring-opening agent, iodide, in complex **11**.

The development of methods for easily replacing the iodide ligand in complex **11** are therefore necessary for providing a better model homogeneous catalyst. In a manner similar to that described for the synthesis of the Fe−PPh_3

(11) Darensbourg, D. J.; Niezgoda, S. A.; Holtcamp, M. W.; Draper, J. D.; Reibenspies, J. H. *Inorg. Chem.* **1997**, *36*, 2426−2432.

derivative, **9**, the tetrafluoroborate analogue of complex **11** was synthesized. Technically, complex **12**, [CpFe(μ-CN)$_2$Zn-(BF$_4$)(THF)]$_2$(μ-dppp), should serve as a good source for providing more active DMC catalysts via subsequent reaction with various sodium salts, e.g., sodium phenoxides. However, the difficulty of removing all of the sodium tetrafluoroborate byproduct is a disadvantage of this synthetic methodology. This simple metal salt contamination must be avoided due to its potential detrimental affect on the copolymerization process. An alternative method to prepare derivative of complex **11** with other nucleophiles attached to zinc would entail the use of protonated iron cyanide complexes in conjunction with zinc amides.[12]

The protonated derivative, HCpFe(CO)(CN)$_2$, was first synthesized by Coffey[13] and has since been crystallographically characterized by us where protonation is shown to occur at the cyanide nitrogen.[14] Despite the synthesis of these derivatives in aqueous solution, no water was found in the crystal structure of the protonated dicyanide. This is beneficial since residual water is detrimental to the copolymerization process and would have to be removed. The reactions of KCpFe(CN)$_2$PPh$_3$ and [KCpFe(CN)$_2$]$_2$(μ-dppp) with excess concentrated HCl in methanol resulted in formation of the protonated analogues, complexes **13** and **14**, H[CpFe(PPh$_3$)(CN)$_2$] and [HCpFe(CN)$_2$]$_2$(μ-dppp), respectively. These protonated metallodicyanides are insoluble under neutral pH conditions in water and most organic solvents and, therefore, preclude obtaining solution NMR data. Solid-state infrared spectra showed that upon protonation the ν(CN) vibrational modes in **13** and **14** shift to higher frequencies as compared to their potassium salts. A similar observation was made with the HCpFe(CO)(CN)$_2$ derivative. The reaction of complex **13** with 1 equiv of Zn[N(SiMe$_3$)$_2$]$_2$ can be visually monitored and shown to yield the silyamide double metal cyanide complex. This derivative is extremely moisture sensitive and decomposes rapidly in THF solution. It was therefore synthesized in situ and directly reacted with 1 equiv of phenol to afford the phenolate complex **15**, [CpFe(PPh$_3$)(μ-CN)$_2$Zn(2,6-OC$_6$H$_3$(*tert*-butyl)$_2$)(THF)]$_2$. The analogous diphosphine-bridged complex **16**, [CpFe(μ-CN)$_2$Zn-(2,6-OC$_6$H$_3$(*tert*-butyl)$_2$)(THF)]$_2$(μ-dppp), was prepared in a similar fashion from the protonated iron dicyanide **14**. Both phenolate complexes, **15** and **16**, have similar ν(CN) frequencies at 2101, 2080 and 2101, 2078 cm^{-1}, respectively.

Copolymerization Reactions. Complex **11** was explored as a catalyst or catalyst precursor for the copolymerization of cyclohexene oxide and carbon dioxide. Although iodide is not a good initiator, this complex was chosen because it was crystallographically well-defined and expected to remain intact under the reaction conditions. This latter expectation was examined by monitoring complex **11** dissolved in α-pinene oxide. α-Pinene oxide was selected because of its similarity to cyclohexene oxide in its binding properties, yet

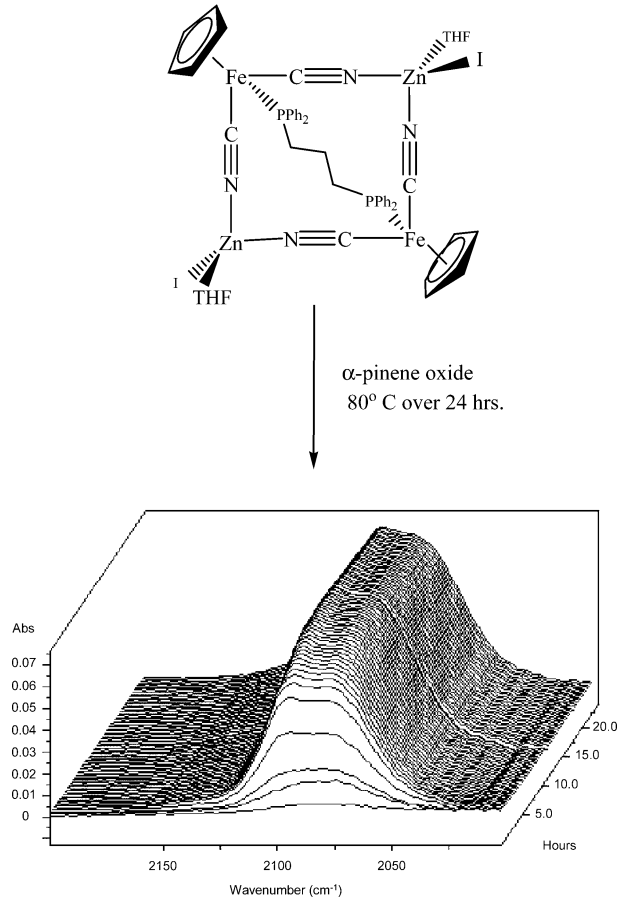

Figure 7. In situ infrared spectra of the ν(CN) of **11** under simulated polymerization conditions with reactant dissolution increasing over the first four scans.

it is an epoxide which is difficult to ring-open and lead to polyether formation.[15] The ν(CN) infrared spectrum of complex **11** at 80 °C was followed in a glass vessel fitted to an in situ ReactIR probe over a 24 h time period. As shown in Figure 7, once the complex completely dissolves in the epoxide, there is *no* change in the ν(CN) band positions or intensities with time, nor do additional ν(CN) bands appear in the spectrum. Hence, this is strong evidence that complex **11** maintains its core structural integrity under the reaction conditions of the copolymerization process.

The copolymerization of cyclohexene oxide and carbon dioxide was carried out as described in the Experimental Section by employing complex **11** (0.15 g, 0.12 mmol) as catalyst. An infrared spectrum in the ν(CO$_2$) region of the crude reaction products obtained in methylene chloride revealed a peak at 1802 cm^{-1} for the cyclic carbonate which was much larger than that of the copolymer at 1750 cm^{-1} (see Figure 8). Interestingly, the cyclic carbonate produced was exclusively the cis isomer as revealed by comparison with an authentic sample synthesized from 1,2-*cis*-cyclohexanediol and triphosgene.[16] Degradation of the growing polymer chain should lead to production of the trans isomer of 7,9-dioxabicyclo[4.3.0]nonan-8-one.[17] A possible mech-

(12) Darensbourg, D. J.; Phelps, A. L.; Adams, M. J.; Yarbrough, J. C. *J. Organomet. Chem.* **2003**, *666*, 49−53.
(13) Coffey, C. E. *Inorg. Nucl. Chem.* **1963**, *25*, 179−185.
(14) Lai, C.-H.; Lee, W.-Z.; Miller, M. L.; Reibenspies, J. H.; Darensbourg, D. J.; Darensbourg, M. Y. *J. Am. Chem. Soc.* **1998**, *120*, 10103−10114.
(15) Darensbourg, D. J.; Wildeson, J. R.; Lewis, S. J.; Yarbrough, J. C. *J. Am. Chem. Soc.* **2002**, *124*, 7075−7083.
(16) Burk, R. M.; Roof, M. B. *Tetrahedron Lett.* **1993**, *34*, 395−398.
(17) Kuran, W.; Listos, T. *Macromol. Chem. Phys.* **1994**, *195*, 977−984.

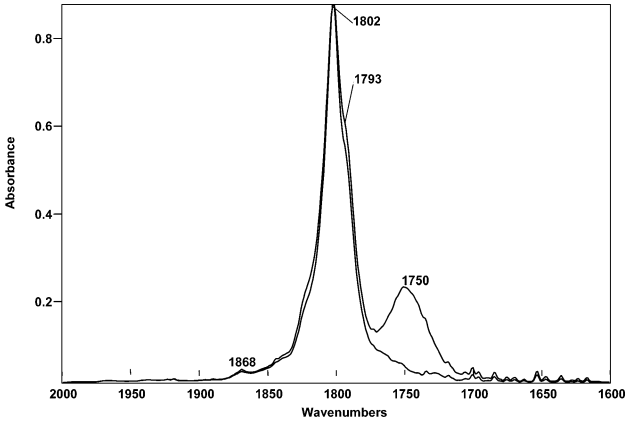

Figure 8. Crude copolymerization product afforded using **11** as the catalyst, with spectrum of an authentic *cis*-cyclohexene carbonate superimposed.

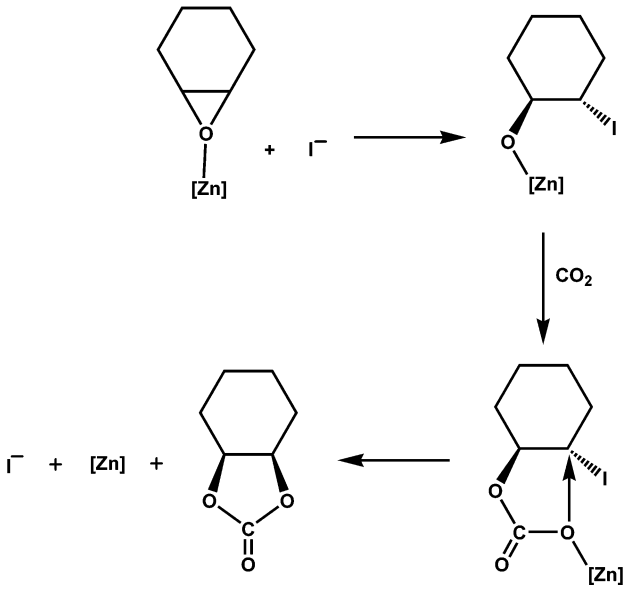

Figure 9. Proposed mechanism for cis cyclic carbonate production.

anism for cis cyclic carbonate formation based on the work of Kisch[18] involves a double inversion at the epoxide carbon center as illustrated in Figure 9. This process is believed to be facilitated by the easily displaced iodide nucleophile. Consequently, cyclic carbonate production occurs at the expense of the enchainment step, thereby accounting for the lack of copolymer formation.

In a similar manner the copolymerization reaction of cyclohexene oxide and carbon dioxide was performed by employing complex **15** as catalyst which contains the better initiator, phenoxide, attached to zinc. As illustrated in Figure 10A the infrared spectrum of the crude reaction product in methylene chloride shows a significant improvement in the quantity of copolymer (88% carbonate linkages via ^{1}H NMR) produced relative to cyclic carbonate. Furthermore, the cyclic carbonate is of the trans configuration as anticipated from degradation of the growing polymer chain. For comparative infrared spectra of cis and trans cyclic cyclohexyl carbonate, see ref 19. The structurally stabilized strapped complex **16**

(18) Dümler, W.; Kisch, H. *Chem. Ber.* **1990**, *123*, 277−283.

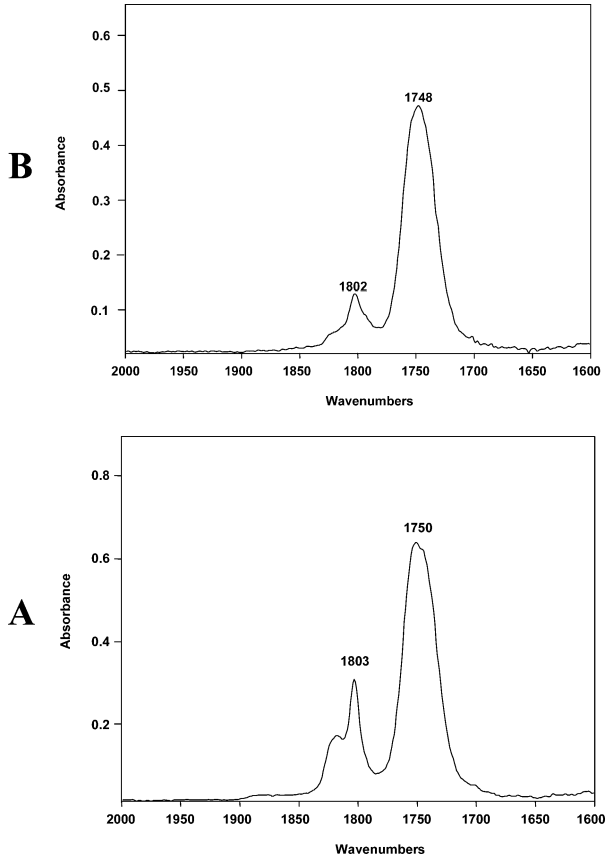

Figure 10. Infrared spectrum of crude reaction product from the copolymerization of cyclohexene oxide and CO_2: (A**)** using complex **15** as catalyst; (B) using complex **16** as catalyst.

was also shown to be a good model for the heterogeneous DMC catalyst. Figure 10B depicts the infrared spectrum of the crude product derived from the copolymerization reaction catalyzed by complex **16**. This spectrum clearly shows trans cyclic carbonate production, along with a sizable amount of copolymer (85% carbonate linkages). Hence, these latter results are similar to the behavior of the patented DMC catalysts; however, it should be noted that they are considerably less active. That is, these homogeneous systems afford yields of copolymer < 10% with TON's < 20 g of polymer/g of Zn. This is to be compared with the Kruper patent (zinc ferricyanide catalyst system) for the copolymerization of cyclohexene oxide/CO_2 carried out under similar reaction conditions, where a 30% conversion (100% copolymer) was reported.[5a]

Concluding Comments

Herein, we have demonstrated that it is possible to synthesize double metal cyanide (DMC) derivatives of iron(II)/zinc(II) which exhibit modest catalytic activity for the coupling of carbon dioxide and epoxides to afford polycarbonates and cyclic carbonates. With utilization of these complexes, in particular the very thermally stable phosphine-bridged derivative (**16**), a working model for the active site in the activated DMC heterogeneous catalysts is

(19) Darensbourg, D. J.; Lewis, S. J.; Rodgers, J. L.; Yarbrough, J. C. *Inorg. Chem.* **2003**, *42*, 581−589.

described. Indeed, this single side strapping by bridging phosphine ligands represents a new approach to stabilizing DMC derivatives. This model invokes a tetrahedrally coordinated zinc center containing two bridging cyanide ligands from the stable anionic iron cyanide moieties, along with an initiator and a site for epoxide binding/activation. A major issue in our catalyst design strategy is the incorporation of the appropriate initiator group. Thus far, we have only been able to fully characterize a DMC derivative containing an iodide as initiator. Hence, there is a need for developing synthetic methods for preparing and structurally defining DMC complexes possessing better initiators, such as azide or methoxide groups. Using heterogeneous zinc glutarate catalysts, Chisholm and co-workers[20] have reported hydroxyl end groups in polypropylene carbonates produced from propylene oxide and CO_2. Similarly, the DMC catalysts in the patent literature are likely to employ OH^- or OR^- initiators on some zinc sites on the basis of their method of activation. It is hoped with proper catalyst design incorporating good initiators all zinc sites could be catalytically active in the homogeneous DMC catalysts. It may also be necessary to fine-tune the electronics of the bridging cyanide ligands by way of the iron center, i.e., using modified cyclopentadienyl ligands and various phosphine/phosphite ligands, to more closely mimic the situation in the heterogeneous catalytic system. These investigations are ongoing in our laboratory.

Experimental Section

Methods and Materials. All manuipulations were carried out using standard Schlenk and drybox techniques under an atmosphere of argon unless otherwise stated. Prior to their use, hexane, diethyl ether, THF, benzene, and toluene were distilled over sodium benzophenone. Methanol was dried by distillation over magnesium turnings and iodine. Acetonitrile was dried by successive distillation over CaH_2 and P_2O_5, whereas dichloromethane was distilled over P_2O_5. All phosphines were purchased from Strem. Zinc iodide and all phenols were obtained from Aldrich. Zinc dust was purchased from Baker Scientific, and nitrosyl tetrafluoroborate was obtained from Lancaster Synthesis Inc. $KCpFe(CN)_2CO$,[13,14] $KCpFe(CN)_2PPh_3$,[10] $[KCpFe(CN)_2]_2(\mu\text{-}Ph_2P(CH_2)_3PPh_2)$,[10] and $Zn(CH_3CN)_4(BF_4)$[21] were prepared using the published procedures.

Physical Measurements. All vibrational studies were carried out on a Mattson 6021 FTIR spectrometer, using a 0.1 mm CaF_2 sealed cell. ^1H and ^{31}P NMR were recorded on a 300 MHz Varian Unity Plus spectrometer (121.4 MHz ^{31}P), with acetonitrile as the solvent unless otherwise stated. Deuterated water was used as the lock solvent, and all spectra were referenced to an 85% phosphoric acid solution. All samples for solid-state ^{15}N and ^{13}C NMR measurements were ground and packed into zirconium oxide rotors and fitted with Kel-F caps, and spectra were recorded at room temperature on a 7.05 T Bruker MSL 300 superconducting spectrometer. The spin rate of the 7 mm MAS probe was controlled by a Bruker controller. Glycine and adamantane were used as external references for all ^{15}N and ^{13}C spectra, respectively. Cross polarization techniques were employed for signal enhancement with pulse widths optimized between 8 and 6 μs. Contract times of 8 μs were used in all cases. Delay times of both ^{15}N and ^{13}C were set to 6 s.

Synthesis of $[CpFe(CO)(\mu\text{-}CN)_2]_2[Zn]\cdot H_2O$, 2. Method I. A 0.2 g (0.83 mmol) amount of $KCpFe(CN)_2(CO)$ in 25 mL of H_2O was added dropwise into a vigorously stirring solution of 0.113 g (0.83 mmol) $ZnCl_2$ over a period of 2 h at room temperature. The turbid yellow reaction mixture was filtered and washed twice with water to remove any remaining starting material salts. Residual water was removed by heating the product under vacuum overnight to yield the yellow powder **2**. Attempts to dissolve **2** in all common solvents failed, and the same results were noted when using CH_3CN instead of water as the reaction solvent. Anal. Calcd for $[CpFe(CO)(\mu\text{-}CN)_2]_2[Zn]\cdot H_2O$: C, 39.59; H, 2.49; N, 11.54; O, 9.89. Found: C, 39.30; H, 2.15; N, 12.16; O, 10.30; Cl, <0.3.

Method II. Complex **2** can also be synthesized from the ZnI_2 salt under aqueous conditions by following the same procedure as described for method I.

Synthesis of $[CpFe(CO)(\mu\text{-}CN)_2ZnI(CH_3CN)]_2$, 3. A slurry of 0.133 g (0.42 mmol) of ZnI_2 in 15 mL of CH_3CN was added to a Schlenk flask containing 0.1 g (0.42 mmol) of $KCpFe(CN)_2(CO)$ at room temperature via cannula. The reaction mixture was stirred for 60 min to afford a yellow solution along with a white precipitate. The solution was filtered through a frit containing Celite to remove the KI byproduct. CH_3CN was removed under vacuum to yield a fine yellow powder of **3**. Anal. Calcd for $C_{20}H_{16}O_2N_6Fe_2Zn_2I_2$ (M_r = 868.6): C, 27.65; H, 1.86; N, 9.68. Found: C, 28.02; H, 1.92; N, 10.32.

Synthesis of $[CpFe(CO)(\mu\text{-}CN)_2Zn(PR_3)(CH_3CN)]_2[BF_4]_2$, Where PR_3 = PPh_2Me (4), PCy_3 (5), and P^tBu_3 (6). These derivatives were all prepared in a similar manner from the appropriate phosphine. In a typical synthesis a solution of 0.4 g (0.99 mmol) of $Zn(CH_3CN)_4(BF_4)_2$ in 15 mL of CH_3CN was added to 0.2 g (0.99 mmol) of PPh_2Me in a Schlenk flask via cannula. The reaction mixture was stirred at ambient temperature for 1 h prior to being transferred to a flask containing 0.24 g (0.99 mmol) of $KCpFe(CN)_2CO$ in 10 mL of acetonitrile. An immediate reaction occurred as evidenced by the formation of a fine white precipitation of KBF_4. The reaction mixture was stirred for an additional 1 h and filtered through a frit containing Celite to remove the salt byproduct. Vacuum removal of the acetonitrile solvent afforded a fine yellow powder of complex **4**. Anal. Calcd for $C_{46}H_{42}Fe_2O_2N_6Zn_2P_2B_2F_8$ (M_r = 1188.9): C, 46.47; H, 3.56; N, 7.07. Found: C, 47.02; H, 3.71; N, 7.22.

Synthesis of $[CpFe(CO)(\mu\text{-}CN)_2Zn(2,4,6\text{-}OC_6H_2(CH_3)_3)(CH_3CN)]_2$, 7. A 0.079 g (0.5 mmol) amount of sodium 2,4,6-trimethylphenoxide in acetonitrile was added to a Schlenk flask containing 0.068 g (0.5 mmol) of $ZnCl_2$ via cannula. The reaction mixture was stirred for 3 h and the precipitate removed by filtration through Celite. The solution was then added to 0.120 g (0.5 mmol) of $KCpFe(CN)_2(CO)$ while stirring at ambient temperature for 1 h. The resulting yellow solution was filtered a second time and evaporated to dryness under vacuum to yield a yellow powder of complex **7**.

Synthesis of $[CpFe(PPh_3)(\mu\text{-}CN)_2ZnI(THF)]_2$, 8. A slurry of 0.067 g (0.21 mmol) of ZnI_2 in 20 mL of CH_3CN was transferred slowly to a Schlenk flask containing 0.1 g (0.21 mmol) of $KCpFe(CN)_2(PPh_3)$ in 10 mL of CH_3CN via cannula. The solution was stirred for 1 h at which point a yellow solution with white precipitate was observed. The solvent was removed under vacuum, and the solid dissolved in THF. The KI precipitate was then removed by filtration through a frit containing Celite. The solvent was evaporated under vacuum to give the yellow solid **8** in 74% yield. Anal.

(20) Chisholm, M. H.; Navarro-Llobet, D.; Zhou, Z. *Macromolecules* **2002**, *35*, 6494−6504.
(21) Kubas, G. J. In *Inorganic Syntheses*; Shriver, D. F., Ed.; John Wiley and Sons: New York, 1979; pp 19, 90−92.

Table 4. X-ray Crystallographic Data for Complexes **8**, **10a,b**, and **11**

	8	**10a**	**10b**	**11**
formula	$C_{58}H_{56}Fe_2I_2N_4O_2P_2Zn_2$	$C_{115}H_{95}Fe_4IN_{11}P_4Zn_3 \cdot 2NC_5H_5AgI_2$	$C_{70}H_{60}Ag_2Fe_2I_4N_8P_2Zn_2$	$C_{45}H_{52}Fe_2I_2N_4O_2P_2Zn_2$
fw	1399.32	2821.30	2041.06	1239.15
cryst system	monoclinic	triclinic	monoclinic	orthorhombic
space group	$P2_1/n$	$P\bar{1}$	$P2_1/c$	Pnma
Z	4	2	4	6
a, Å	10.936(4)	14.240(4)	13.415(4)	29.029(11)
b, Å	15.982(6)	16.089(5)	11.005(3)	18.924(7)
c, Å	16.338(6)	17.644(5)	25.062(7)	9.052(4)
α, deg		63.302(6)		
β, deg	90.362(8)	69.002(6)	104.232(5)	
γ, deg		79.220(6)		
V, Å^3	2855.3(19)	3370.1(17)	3586.4(18)	4973(3)
d_{calcd}, g/cm^3	1.627	1.907	1.890	2.077
temp, K	110(2)	110(2)	100(2)	293(2)
wavelength, Å	0.710 73	0.710 73	0.710 73	0.710 73
abs coeff, mm^{-1}	2.509	3.560	3.399	4.282
goodness of fit on F^2	1.641	1.161	0.824	1.020
R,[a] %	20.84	18.38	2.29	5.41
R_w,[b] %	51.87	45.00	3.89	12.76

[a] $R = \Sigma|F_o| - |F_c|/\Sigma|F_o|$. [b] $R_w = \{[\Sigma w(F_o^2 - F_c^2)^2]/[\Sigma w(F_o^2)^2]\}^{1/2}$.

Calcd for $C_{58}H_{56}Fe_2Zn_2P_2N_4I_2O_2$ (M_r = 1399.3): C, 49.78; H, 4.03; N, 4.00. Found, C, 51.02; H, 4.17; N, 4.37.

Synthesis of [CpFe(PPh$_3$)(*μ*-CN)$_2$Zn(BF$_4$)(CH$_3$CN)]$_2$, 9. A solution of 0.1 g (0.25 mmol) of Zn(CH$_3$CN)$_4$(BF$_4$)$_2$ in 15 mL of CH$_3$CN was transferred to a Schlenk flask containing 0.118 g (0.25 mmol) of KCpFe(CN)$_2$(PPh$_3$) in 10 mL of CH$_3$CN via cannula. A color change from orange to yellow was seen as the reaction proceeded for 1 h, with no appearance of a precipitate. The solution was evaporated to dryness to yield the yellow solid **9** along with the residual KBF$_4$ byproduct.

Synthesis of [{CpFe(PPh$_3$)(*μ*-CN)$_2$Zn(NC$_5$H$_5$)}$_2${CpFe(PPh$_3$)-(*μ*-CN)$_2$}$_2$ZnI(NC$_5$H$_5$)][AgI$_2$], 10a, and [CpFe(*μ*-CN)$_2$(PPh$_3$)Zn-(NC$_5$H$_5$)$_2$]$_2$[AgI$_2$]$_2$, 10b. A slurry of 0.083 g (0.26 mmol) of ZnI$_2$ in 15 mL of CH$_3$CN was transferred via cannula to a Schlenk flask containing 0.123 g (0.26 mmol) of KCpFe(CN)$_2$(PPh$_3$) in 15 mL of CH$_3$CN. The reaction mixture was stirred for 2 h at room temperature. The KI precipitate was removed by filtration, and the solvent was removed under vacuum. The solid was then dissolved in 20 mL of THF and transferred to a Schlenk flask charged with 0.043 g (0.26 mmol) of AgOOCCH$_3$ via cannula and stirred for 1 h. The solution was filtered through a frit containing Celite to remove the AgI precipitate and evaporated to dryness under vacuum. The yellow solid was then dissolved in pyridine to form the polymeric complex **10a**. Compound **10b** was crystallized from the same solution as **10a**, with the only exception being the length of time taken for crystal growth.

Synthesis of [CpFe(*μ*-CN)$_2$ZnI(THF)]$_2$(*μ*-dppp), 11. A slurry of 0.076 g (0.24 mmol) of ZnI$_2$ in 20 mL of CH$_3$CN was transferred to a Schlenk flask containing 0.1 g (0.12 mmol) of [KCpFe(CN)$_2$]$_2$-(*μ*-dppp) in 10 mL of CH$_3$CN via cannula. The reaction was stirred at room temperature for 2 h to give a yellow solution along with a precipitate. The solvent was removed under vacuum, and the solid was dissolved in THF. The solution was filtered through a frit containing Celite and the solvent removed under vacuum to give the yellow solid of **11**. X-ray-quality crystals of **11** were obtained from THF/hexane at −20 °C. Anal. Calcd for $C_{45}H_{52}Fe_2I_2N_4O_2P_2$-$Zn_2$ (M_r = 1239.15): C, 43.62; H, 4.23; N, 4.52. Found: C, 43.87; H, 4.31; N, 4.67.

Synthesis of [CpFe(*μ*-CN)$_2$Zn(BF$_4$)(THF)]$_2$(*μ*-dppp), 12. A solution of 0.45 g (1.1 mmol) of Zn(CH$_3$CN)$_4$(BF$_4$)$_2$ in 15 mL of CH$_3$CN was added dropwise to a slurry of [KCpFe(CN)$_2$]$_2$(*μ*-dppp) in 10 mL of CH$_3$CN via cannula. The reaction mixture was stirred at room temperature for 4 h to afford a turbid yellow mixture. The solvent was removed under vacuum, and the solid redissolved in THF leaving behind a precipitate which was separated by filtration through a frit containing Celite. The solvent was evaporated under vacuum to give a yellow powder of complex **12** in 64% yield.

Synthesis of H[CpFe(PPh$_3$)(CN)$_2$], 13. An excess (0.7 mL) of degassed concentrated HCl was added to a flask containing 0.2 g (0.42 mmol) of KCpFe(CN)$_2$(PPh$_3$) in 10 mL of MeOH while stirring at room temperature. Approximately 50 mL of degassed H$_2$O was added to the flask after 1 h resulting in the formation of a yellow precipitate. The solution was decanted via cannula, and the precipitate was washed repeatedly with H$_2$O. The product was then washed with MeOH and dried under vacuum to give a yellow powder of **13** in 83% yield. Anal. Calcd for $C_{25}H_{21}N_2PFe$ (M_r = 436.27): C, 68.83; H, 4.85. Found: C, 68.24; H, 5.01.

Synthesis of [HCpFe(CN)$_2$]$_2$(*μ*-dppp), 14. An excess (1.0 mL) of degassed concentrated HCl was added to a flask containing 0.4 g (0.48 mmol) of [KCpFe(CN)$_2$]$_2$(*μ*-dppp) in 10 mL of MeOH while stirring at room temperature. To the resulting green solution approximately 50 mL of H$_2$O was added to afford a yellow precipitate. The solution was decanted via cannula, and the precipitate was washed repeatedly with H$_2$O. The product was then washed with Et$_2$O and dried under vacuum to give a yellow powder of **14** in 89% yield. Anal. Calcd for $C_{41}H_{38}N_4Fe_2P_2$ (M_r = 760.4): C, 64.76; H, 5.04. Found: C, 65.01; H, 4.93.

Synthesis of [CpFe(PPh$_3$)(*μ*-CN)$_2$Zn(2,6-OC$_6$H$_3$(*tert*-butyl)$_2$)-(THF)]$_2$, 15. A 0.035 g (0.09 mmol) amount of Zn[N(SiMe$_3$)$_2$]$_2$ in 10 mL of THF was transferred to a Schlenk flask containing 0.04 g (0.09 mmol) of **13** in 10 mL of THF via cannula. The reaction mixture was stirred at room temperature for 15 min. A solution of 0.019 g (0.09 mmol) of 2,6-di-*tert*-butylphenol in 5 mL of THF was added via cannula to the reaction mixture, which was stirred for 30 min. The yellow solution was evaporated to dryness under vacuum to provide a yellow powder of complex **15**.

Synthesis of [CpFe(*μ*-CN)$_2$Zn(2,6-OC$_6$H$_3$(*tert*-butyl)$_2$)(THF)]$_2$-(*μ*-dppp), 16. A 0.071 g (0.18 mmol) amount of Zn[N(SiMe$_3$)$_2$]$_2$ in 10 mL of THF was transferred to a Schlenk flask containing 0.07 g (0.09 mmol) of **14** in 10 mL of THF via cannula. The reaction mixture was stirred at room temperature for 15 min. A solution of 0.037 g (0.18 mmol) of 2,6-di-*tert*-butylphenol in 5 mL of THF was added via cannula to the reaction mixture, which was stirred for 30 min. The yellow solution was evaporated to dryness under vacuum to give a yellow powder of complex **16**.

Polymerization Reactions. A sample of catalyst (generally 0.10−0.15 g) was dissolved in 20 mL of epoxide. The solution was loaded via an injection port into a 300 mL stainless steel Parr autoclave, which had previously been dried overnight under vacuum at 80 °C. The reactor was pressurized to 52 bar with carbon dioxide and heated to 80 °C. After a period of time (usually 24 h), the reactor was cooled and opened and the products were isolated by dissolution in CH_2Cl_2. The crude reaction mixture was initially analyzed for polycarbonate and cyclic carbonate by infrared spectroscopy in the $\nu(CO_2)$ region. The copolymer was characterized by ^{1}H NMR spectroscopy, where protons adjacent to carbonate linkages afford a signal at 4.6 ppm, while the polyethers appear at 3.5 ppm.

X-ray Crystallography. Yellow single crystals of compounds **8**, **10a,b**, and **11** were coated with Paratone and mounted on a glass fiber using Apiezon grease at room temperature. The crystals were then placed on a Bruker Smart 1000 diffractometer equipped with a CCD detector in a nitrogen cold stream maintained at 110 K. More than a hemisphere of data was collected on each crystal over three batches of exposures using Mo Kα radiation (λ = 0.710 73 Å). A fourth set of data was measured and compared to the initial set to monitor and correct for decay, which was negligible in all cases. Details of crystal data collected on compounds **8**, **10a,b**, and **11** are provided in Table 4.

Systematic absences and intensity statistics were used in space group determination. All structures were solved using direct methods. Anisotropic structure refinements were achieved using full-matrix least-squares techniques on all non-hydrogen atoms. All hydrogen atoms were placed in idealized positions based on hybridization, with isotropic thermal parameters fixed at 1.2 or 1.5 times the value of the attached atom. All atom scattering factors were obtained from the International Tables for X-ray Crystallography, Vol. C.

Structure solutions for compounds **8**, **10a,b**, and **11** were obtained using the following programs: data collection, SMART;[22] cell refinement, SAINT;[23] data reduction, SAINT;[23] structure solution, SHELXTL-Plus;[24] molecular graphics, SHELXTL-Plus.[25]

Acknowledgment. Financial support from the National Science Foundation (Grant Nos. CHE 99-10342 and CHE 02-34860 and CHE 98-07975 for purchase of X-ray equipment), the Robert A. Welch Foundation, and the Texas Advanced Research Technology Program (Grant No. 0390-1999) is greatly appreciated.

Supporting Information Available: Complete details of the X-ray diffraction study of complexes **8**, **10a,b**, and **11** (CIF). This material is available free of charge via the Internet at http://pubs.acs.org.

IC0347900

(22) *SMART 1000 CCD*; Bruker Analytical X-ray Systems: Madison, WI, 1999.
(23) *SAINT-Plus*, version 6.02; Bruker Analytical X-ray Systems: Madison, WI. 1999.
(24) Sheldrick, G. *SHELXS-86 Program for Crystal Structure Solution*; Institut fur Anorganische Chemie der Universitat: Gottingen, Germany, 1986.
(25) *SHELXTL*, version 5.0; Bruker Analytical X-ray Systems: Madison, WI, 1999.